AMERICAN SOCIETY FOR MICROBIOLOGY | Antimicrobial Agents and Chemotherapy®

MECHANISMS OF RESISTANCE

The Essential Role of Hypermutation in Rapid Adaptation to Antibiotic Stress

Heer H. Mehta,[a] Amy G. Prater,[a] Kathryn Beabout,[a]* Ryan A. L. Elworth,[b] Mark Karavis,[c] Henry S. Gibbons,[c] Yousif Shamoo[a]

[a]Department of Biosciences, Rice University, Houston, Texas, USA
[b]Department of Computer Science, Rice University, Houston, Texas, USA
[c]U.S. Army Edgewood Chemical Biological Center, Aberdeen Proving Ground, Maryland, USA

ABSTRACT A common outcome of antibiotic exposure in patients and *in vitro* is the evolution of a hypermutator phenotype that enables rapid adaptation by pathogens. While hypermutation is a robust mechanism for rapid adaptation, it requires trade-offs between the adaptive mutations and the more common "hitchhiker" mutations that accumulate from the increased mutation rate. Using quantitative experimental evolution, we examined the role of hypermutation in driving the adaptation of *Pseudomonas aeruginosa* to colistin. Metagenomic deep sequencing revealed 2,657 mutations at ≥5% frequency in 1,197 genes and 761 mutations in 29 endpoint isolates. By combining genomic information, phylogenetic analyses, and statistical tests, we showed that evolutionary trajectories leading to resistance could be reliably discerned. In addition to known alleles such as *pmrB,* hypermutation allowed identification of additional adaptive alleles with epistatic relationships. Although hypermutation provided a short-term fitness benefit, it was detrimental to overall fitness. Alarmingly, a small fraction of the colistin-adapted population remained colistin susceptible and escaped hypermutation. In a clinical population, such cells could play a role in reestablishing infection upon withdrawal of colistin. We present here a framework for evaluating the complex evolutionary trajectories of hypermutators that applies to both current and emerging pathogen populations.

KEYWORDS antibiotic stress, experimental evolution, hypermutation

Hypermutation is a phenomenon that is often observed in clinical isolates of pathogenic species (1–3). The opportunistic pathogen *Pseudomonas aeruginosa* is a common nosocomial pathogen affecting immunocompromised patients, especially those with cystic fibrosis (CF). Thirty percent to 54% of CF patients infected with *P. aeruginosa* are colonized by hypermutator strains that are associated with reduced lung function and chronic infections (4–6). During infection, *P. aeruginosa* also forms persistent and difficult-to-clear biofilms that are known to exhibit reduced susceptibility to antimicrobials (7, 8). *P. aeruginosa* also exhibits great metabolic and genetic plasticity, allowing it to readily acquire resistance to antibiotics (9). Resistance to the drug of last resort, a cationic antimicrobial peptide (CAP) called colistin (polymyxin E), has been observed and has been associated with hypermutation (10–13).

Mutation acquisition during selection is dependent on mutation supply, which can be boosted by hypermutation (14, 15). The typical path leading to a hypermutator phenotype is mutations in the DNA repair system, including the MutS/MutL class of proteins (14, 16, 17). The increase in mutation supply increases the rate at which bacteria become resistant; thus, hypermutators explore the adaptive evolutionary trajectories leading to resistance more rapidly than with nonhypermutators. Interestingly, the dramatic increase in mutation rate also means that many nonadaptive mutations accumulate and are carried along as "hitchhikers" that in the long run are

Citation Mehta HH, Prater AG, Beabout K, Elworth RAL, Karavis M, Gibbons HS, Shamoo Y. 2019. The essential role of hypermutation in rapid adaptation to antibiotic stress. Antimicrob Agents Chemother 63:e00744-19. https://doi.org/10.1128/AAC.00744-19.

Address correspondence to Yousif Shamoo, shamoo@rice.edu.

* Present address: Kathryn Beabout, Air Force Research Laboratory, Wright-Patterson AFB, Ohio, USA.

Received 9 April 2019
Returned for modification 17 April 2019
Accepted 19 April 2019

Accepted manuscript posted online 29 April 2019
Published 24 June 2019

likely to decrease the overall fitness of the organisms under nonselective conditions (18, 19). Nevertheless, hypermutation provides a swift strategy for cells undergoing stress to acquire adaptive mutations before they go extinct.

Experimental evolution is a powerful approach to understanding the genetic and biochemical basis for antibiotic resistance (16, 20–26). In this work, *P. aeruginosa* PAO1 was evolved to colistin resistance as a continuous culture in a bioreactor where the population was constantly maintained at mid-exponential phase in the presence of subinhibitory drug concentrations (24). The observation of hypermutation, accompanied by a dramatic increase in mutation rate among the evolving PAO1 population, presented both challenges and opportunities for understanding the evolution of colistin resistance. The potential benefits of this complex data set, however, were equally clear. Hypermutation generated an extensive, if not nearly exhaustive, survey of the accessible evolutionary trajectories leading to colistin resistance.

We used a combination of phylogenetic and statistical approaches to sort through these complex data, discern truly adaptive alleles from hitchhikers, and infer not just the major genetic changes associated with colistin resistance but also those alleles that in combination with the major players were essential to produce the high MICs observed in many clinical isolates (12, 27). Our work has benefited strongly from a series of clinical and *in vitro* experimental evolution studies that have identified many of the major contributors to colistin resistance in *P. aeruginosa* (10, 12, 13, 27, 28).

Taken together, our work provides a comprehensive survey of the alleles responsible for *P. aeruginosa* resistance to colistin and perhaps, more importantly, a means to examine future hypermutators in less-well-characterized or emerging pathogens. The increased mutation rate of hypermutators provides a major adaptive advantage to this pathogen during exposure to colistin. This highlights the strength of hypermutation as an adaptive strategy during exposure to stress and the adaptability of *P. aeruginosa* to survive under such conditions.

RESULTS

Hypermutator variants of *P. aeruginosa* emerge rapidly after colistin exposure during continuous experimental evolution. *P. aeruginosa* PAO1 was propagated in the presence of colistin as a continuous culture in a bioreactor using quantitative experimental evolution (24). The starting MIC of colistin for PAO1 varied from 1 to 2 μg/ml. Over the course of experiment, the PAO1 population was exposed to increasing, but subinhibitory, concentrations of colistin to a final concentration of 16 μg/ml colistin, which is four times higher than the clinical breakpoint for resistance of *P. aeruginosa* to colistin (MIC, $\geq$4 μg/ml) (29). Genomic DNA from each daily population was prepared for metagenomic deep sequencing. At the end of the experiment, the final population was serially diluted and spread on a nonselective growth medium for the isolation of endpoint isolates for whole-genome sequencing. The endpoint isolates produced colonies of diverse morphologies (see File S1 in the supplemental material) consistent with the selection of a highly polymorphic population within the bioreactor experiments, and this was consistent across duplicate experiments. Single colonies isolated from the final populations ranged from being totally susceptible to totally resistant to colistin, which is also consistent with a diverse polymorphic population (Fig. S1b and Table S1). Twenty-nine endpoint isolates were selected for whole-genome sequencing.

Of the 29 sequenced isolates, 25 contained mutations within *mutS,* the gene encoding the DNA mismatch repair enzyme MutS (Fig. 1) (30). Those endpoint isolates that had acquired *mutS* mutations had 44 to 92 mutations each, while strains without mutations in *mutS* had 5 to 9 mutations, showing that mutations within *mutS* correlated with increased genetic diversity. Metagenomic deep sequencing of daily populations showed that on day 10 of adaptation during both replicates 1 and 2 (corresponding to 1.75 μg/ml colistin in replicate 1 and 2 μg/ml colistin in replicate 2), mutations were observed readily in *mutS* (Fig. 1). While the majority of the population contained mutations within *mutS*, a fraction of the final population did not become hypermuta-

Mutation in *mutS*	Effect of mutation	Frequency on final day of adaptation	Mutational trajectory
Replicate 1:			
L142P (T -> C at nucleotide position 425)	Point mutation in connector domain of MutS	78.7%	
1bp deletion at nucleotide position 1745	Premature stop codon at amino acid position 609 (Wild type MutS=855 amino acids)	6.7%	
Replicate 2:			
9 bp deletion (nucleotides 1536 to 1544)	Deletion of amino acids 512-514 in the lever domain of MutS	92.4%	
10 bp deletion (nucleotides 2520 to 2529)	Extends open reading frame and alters last 16 amino acids of MutS	0%	

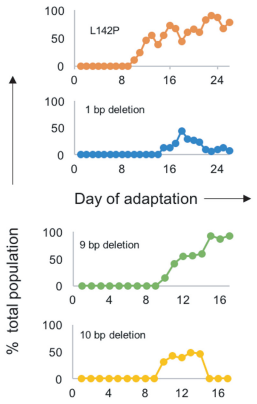

FIG 1 *mutS* mutations observed during adaptation of *P. aeruginosa* populations to colistin. In duplicate experiments (replicates 1 and 2), mutations were seen in the *mutS* gene. The specific mutations identified, their effect on MutS, and their abundances in the evolved populations are indicated (mutation detection cutoff, 5%). The last column shows the frequency for each *mutS* mutation over the course of evolution. The *x* axis shows the day of adaptation (26 days in replicate 1 and 17 days in replicate 2), and the *y* axis indicates the percentage of the total population that possessed the mutation.

tors (14.6% in replicate 1 and 7.6% in replicate 2). In a control experiment involving adaptation of PAO1 in the absence of colistin using the same procedure, it was observed that the population also evolved as a hypermutator due a single point mutation in the *mutS* gene that became detectable on day 11 and spread to 45.1% of the population at the end of adaptation. This population, however, was completely susceptible to colistin (data not shown).

As expected, acquisition of the *mutS* mutations was accompanied by a rapid increase in mutation frequency in the total evolving populations. As seen in Fig. 2, the starting population on day 1 of colistin adaptation in both replicates, as well as the control population, had a basal level of diversity. Aside from the underlying diversity in the population, what is apparent from Fig. 2 is that as soon as *mutS* mutations arose in both of the evolving populations (indicated by red stars), the populations started accumulating more mutations that rose to higher frequencies than mutations contributing to the basal diversity in the population. This was accompanied by increased nonsusceptibility of the total population to colistin in the colistin evolved populations but not the control population. Interestingly, lineages derived from replicate 1 *mutS* with a 1-bp deletion that introduces a premature stop codon at residue 609 and replicate 2 *mutS* with a 10-bp deletion that alters the last 16 amino acids both go to extinction, demonstrating that hypermutation, while increasing the probability of finding successful evolutionary trajectories, does not guarantee success. It may also be hypothesized that the unsuccessful *mutS* mutant lineages have stronger mutator phenotypes that accumulate deleterious mutations more rapidly, leading to a faster decrease in overall fitness than with the more successful *mutS* mutants in replicates 1 and 2.

Evolutionary relationship of endpoint isolates highlights the role of secondary mutations in resistance. Phylogenetic trees were constructed to identify the linkages of mutations within the endpoint isolates (Fig. 3). The 29 sequenced endpoint isolates had cumulatively acquired 761 total mutations affecting 563 genes. It was interesting to note that in duplicate colistin adaptation experiments, isolates that did not acquire *mutS* mutations were phylogenetically closely related to the ancestor and had no increase in colistin resistance. The lack of success in achieving high levels of colistin tolerance by the nonhypermutators highlights the higher efficiency of sampling the

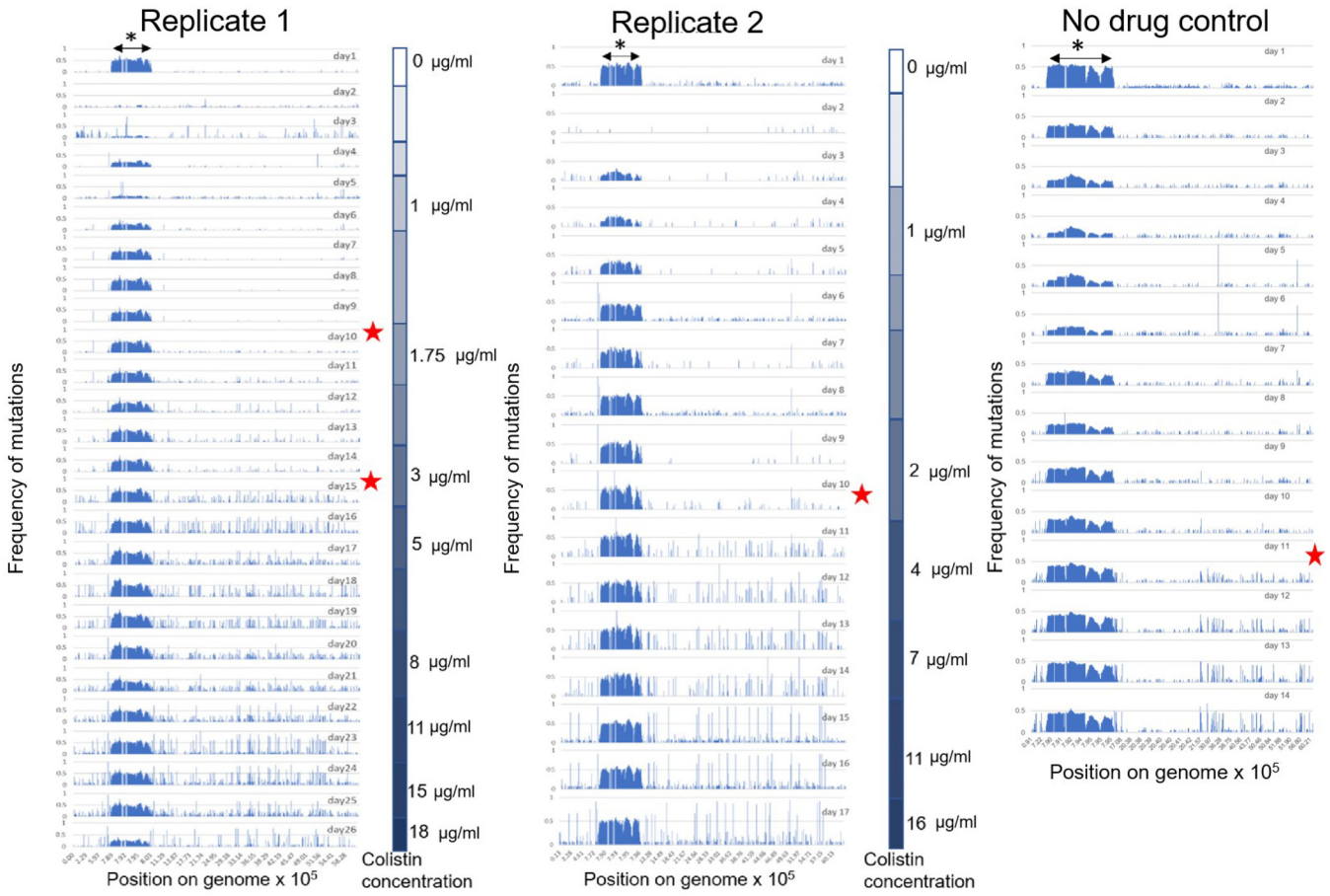

FIG 2 Single nucleotide polymorphism (SNP) map of the PAO1 populations evolving to colistin (replicates 1 and 2) and evolving without colistin (no-drug control). For ease of comparison, the graphs represent a linearized genome of PAO1 with SNP positions indicated on the *x* axis. The *x* axis is not distributed evenly but denotes positions on the genome carrying mutations. This is done to highlight regions of the genome with higher mutation density. The *y* axis is the frequency of the mutation in the total population. For each adaptation experiment, graphs of daily sampled populations are stacked (26 days of evolution for replicate 1, 17 days for replicate 2, and 14 days for the no-drug control). Red stars indicate days on which *mutS* mutations arose in each population. The color gradients on the right side of each graph for replicates 1 and 2 show the stepwise increase in colistin concentrations experienced by the populations during adaptation. The increased genetic diversity in the region from 7.8×10^5 to 8×10^5 bp on the PAO1 genome can be attributed to the Pf4 phage island (indicated by asterisk), the details of which are provided in File S1.

potential evolutionary trajectories by strains with elevated mutation rates. Endpoint isolates containing *mutS* mutations had undergone considerable divergence, with each branch varying substantially in the total number and type of mutations. It was evident that being a hypermutator alone was not sufficient to acquire resistance. Isolates like I1-6 and I1-76 that had $MutS^{L142P}$ were still susceptible (MIC, 2 μg/ml), and thus, while mutations to *mutS* are drivers for adaptation, they are not directly responsible for increased colistin resistance. This is further underscored by the susceptibility of the hypermutator control population.

The highest levels of resistance were achieved by endpoint isolates that emerged from branches containing mutations in the *pmrAB* genes. Previous studies in *P. aeruginosa* have identified the role of PmrAB in resistance to cationic antimicrobial peptides (CAPs) (31, 32). In Fig. 3a, the branch with the initial *pmrB* mutation diverged into several branches leading to endpoint isolates that varied in MICs from 16 to 128 μg/ml. Similarly, in Fig. 3b, different endpoint isolates diverging from the same *pmrA* or *pmrB* branch had different colistin MICs. This suggested that although mutations in *pmrAB* were required for achieving resistance, additional mutations in resistant endpoint isolates were playing an essential role in increasing resistance to colistin.

Hypermutation reveals challenges in distinguishing adaptive mutations from hitchhikers. As the final populations of experimental evolution were dominated by

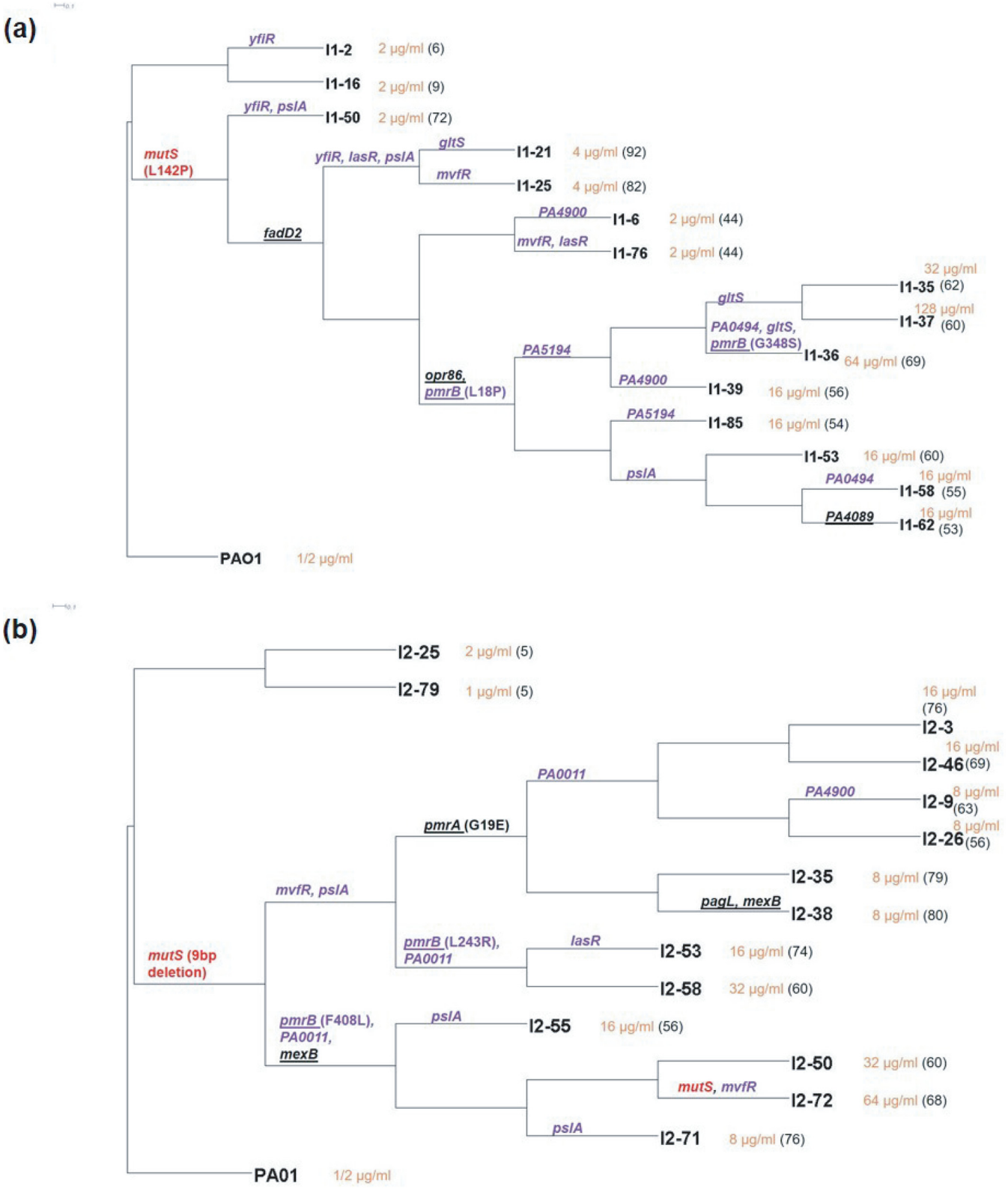

FIG 3 Phylogenetic trees for endpoint isolates obtained from experimental evolution replicate 1 (a) and replicate 2 (b). PAO1 is the ancestor strain. Isolate names are at the right side of each branch. Orange text following the isolate name denotes its colistin MIC, and in parentheses is the total number of mutations identified in that particular isolate. Branches with mutations in putative targets identified in this study have names of the mutated genes on them. Targets in purple text were identified by Fisher's exact test of endpoint isolates, and the targets underlined were common among our study and other polymyxin resistance studies. *mutS* mutations are identified in red text. The large number of mutations per hypermutator lineage precludes their complete inclusion in these phylogenetic trees. The complete list of mutations in each endpoint isolate can be found in Data Set S1.

TABLE 1 Putative targets involved in colistin resistance in PAO1 based on mutations observed in endpoint isolates[a]

Gene name by use	Mutation(s) identified in endpoint isolates	*P* value (Fisher's exact test)	Function (reference[s])
Fisher's exact test of endpoint isolates			
mvfR	Y77H, V162A, L6P, V9V	8.39e−6	Quorum sensing and virulence regulator
pmrB	L18P, G348S, L243R, F408L	3.4e−5	Two-component system involved in cationic antimicrobial sensing and resistance (32)
pslA	Frameshifts, 700-bp deletion, G364D, R229C, Y268H	3.43e−5	Exopolysaccharide involved in biofilm formation; involved in biofilm resistance to antibiotics (53)
yfiR	L183P, C71S, Y58C	5.43e−5	Part of c-di-GMP regulator system involved in biofilm formation.
lasR	L118P, G235D, T115A	1.06e−4	Quorum sensing regulator
PA5194	W64*, G227D, W239*	1.46e−4	LpxT, phosphorylation of lipid A
PA0011	Frameshifts, W33*	1.96e−4	2-Hydroxylauroyl transferase, transfers 2-hydroxylaurate to C-2 position of lipid A
gltS	A194V, G351S, L126L	4.86e−4	Glutamate/sodium symporter
PA4900	L321P, P339P, Q4*	6.45e−4	Probable major facilitator superfamily transporter
PA0494	A44V, P56L, Y201Y	6.96e−4	Probable acyl-CoA carboxylase subunit
From isolates observed in other polymyxin resistance studies of *P. aeruginosa*			
pmrAB	G19E, L18P, G348S, L243R, F408L		Two-component system involved in cationic antimicrobial sensing and resistance (12, 13, 28, 32)
PA5194	W64*, G227D, W239*		Lipid a kinase, adds phosphate group to lipid A (12)
fadD2	Q245R		Long-chain fatty acid CoA ligase (12)
opr86	D535N		Outer membrane protein (12)
PA4089	G105D		Probable short-chain dehydrogenase involved in fatty acid biosynthesis (28)
pagL	D118G		Lipid A deacylation, upregulated by polymyxin (36)
mexB	T242A, T295A		RND multidrug efflux transporter (12)[b]

[a]Although *migA* was identified as significant by Fisher's exact test, it was mutated in the control population that was not exposed to colistin and was hence considered to be involved in adaptation to the bioreactor rather than the drug.
[b]RND, resistance nodulation division.

cells with mutator phenotypes, classical genetic approaches for the validation of adaptive alleles, such as reintroducing the proposed changes into a clean genomic background, were effectively impossible (with an average of 60 mutations per hypermutator endpoint isolate, there were 60! possible combinations of mutations) and required a different approach. While hypermutation introduced a large number of nonadaptive hitchhiker alleles into both the metagenomic and endpoint isolate genomic data, the extensive mutational saturation offered a methodological path forward. A statistical approach was used to identify potentially adaptive genes based on the concept that if a larger-than-expected number of mutations in the same gene across various endpoint isolates from both colistin-adapted populations was identified, those genes were more likely to be adaptive (16). Under the null hypothesis that all mutations were randomly distributed across the genome, 11 genes were identified that were mutated more frequently than expected in the endpoint isolates using Fisher's exact test (Table 1). A total of 563 genes were mutated in the 29 sequenced endpoint isolates. By plotting the number of mutations per gene versus the percentage of endpoint isolates having a mutation in that gene (Fig. 4), it was observed that some of the statistically significant genes ($P < 0.001$) were located on the top-right quadrant. The exception to this was *mutS*. Although *mutS* was seen in 25 of the 29 sequenced endpoint isolates that have a total of 3 unique mutations in this gene, the *mutS* gene itself was sufficiently long (2,568 bp) so that it did not meet the *P* value cutoff of 0.001 for being called significant. If a gene is very long or if a single mutation or small subset of mutations are the only possible adaptive changes in that gene, it may not rise above the required *P* value according to Fisher's exact test. This highlights a shortcoming of this particular approach and explains why we combine it with other methods (discussed below) to increase the overall success in identifying adaptive alleles.

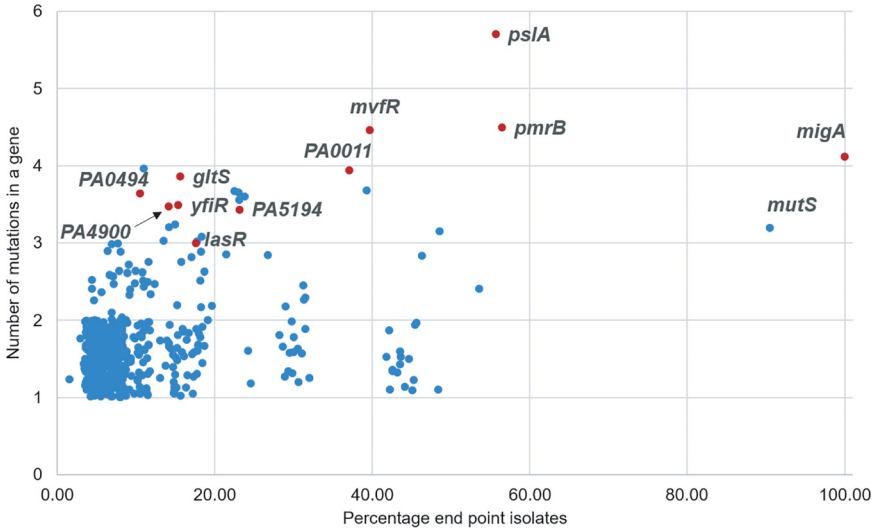

FIG 4 Genes mutated more frequently than expected identified using Fisher's exact test. The number of mutations identified within a single gene among the 29 sequenced endpoint isolates was plotted against the percentage of endpoint isolates containing a mutation in that gene. Genes identified as significant with a *P* value less than 0.001 in Fisher's exact test are highlighted in red. False noise has been added to the data points to separate them on the graph. A detailed analysis of this graph is provided in File S1.

Among the daily populations evolving to colistin resistance from both replicates, 1,197 genes were mutated, and a total of 2,657 mutations were identified at ≥5% frequency. When this same test was performed on these mutations, 41 genes were identified as significant (Table 2). Among these 41 genes, four were also identified in Fisher's exact test of the endpoint isolates (*pmrB, PA0011, migA,* and *pslA*). A comparison of these alleles with alleles mutated in the control population showed that *migA* acquired mutations even in the absence of colistin, suggesting that mutations in *migA* were not a response to colistin but were associated with PAO1 adapting to the bioreactor environment. *pmrA,* which is known to be involved in resistance, was not identified as a significant gene in the endpoint isolates but was in the daily populations. The power of this test could certainly be increased by having data from multiple evolving populations instead of the 2 replicates conducted in this work. Taken together, however, the cumulative data from the 2 populations and 29 endpoint isolates provide an extensive list of genes that potentially play a role in colistin resistance.

Identification of additional genes associated with colistin resistance. Previous studies have been conducted to identify genetic changes leading to polymyxin resistance in *P. aeruginosa* (11–13, 27, 28, 32–34). Since resistance has often been associated with hypermutation (12, 13), which leads to the accumulation of a large number of nonadaptive hitchhiker mutations, not all mutations can be implicated in resistance. However, if the same gene is mutated during adaptation to polymyxin in different studies that use different experimental conditions, it is more likely an adaptative allele than a hitchhiker. We identified such genes that were found to be mutated in our study as well as previous studies and arranged them in the following functional groups: a two-component system, *pmrAB*, lipopolysaccharide modification and biosynthesis genes (*pagL* and *PA5194*), long-chain fatty acid coenzyme A (CoA) ligase (*fadD2*), outer membrane protein (*oprB6*), probable short-chain dehydrogenase (*PA4089*), and multidrug efflux transporter (*mexB*). While the role of some of these genes in polymyxin resistance has been validated (for example, in *pmrAB*, *oprB6, PA5194*, *pagL,* and *mexB*), others have not been previously associated with resistance (12, 13, 28, 32, 35, 36). While *migA* has been identified in colistin resistance-evolved *P. aeruginosa* samples in other studies (12, 13) and in this work, the presence of *migA* mutations in the control population suggests that it most likely plays a role in adaptation to the medium or growth conditions rather than the antibiotic. The other targets were mapped on the

TABLE 2 Candidate colistin resistance genes identified as significant by Fisher's exact test of daily populations[a]

Gene by function[b]	No. of mutation events	Function	*P* value	Comments
LPS modification				
pmrB	19	Sensor kinase of two-component system, PmrAB	4.41E−22	Also identified in Fisher's exact test of endpoint isolates
PA0011	9	Probable 2-OH-lauroyltransferase	3.19E−10	Also identified in Fisher's exact test of endpoint isolates
pmrA	4	Response regulator of two-component system, PmrAB	2.15E−04	Involved in polymyxin resistance (54)
Biofilm synthesis				
pelA	13	Modification and secretion system for Pel polysaccharide-dependent biofilm	6.44E−10	Mutations in Pel polysaccharide genes also identified previously (10, 12)
pslA	8	Psl polysaccharide synthesis and biofilm formation	2.85E−07	Also identified in Fisher's exact test of endpoint isolates
pslN	4	Involved in Psl biosynthesis	9.81E−04	Part of operon containing *pslA*
Unknown role				
wspA	9	Probable chemotaxis transducer	5.53E−08	
PA1336	8	Probable two-component sensor	2.24E−06	
PA3272	11	Probable ATP-dependent DNA helicase	4.02E−06	Mutation in PA3272 also identified previously (12)
ostA	9	Organic solvent tolerance protein	4.28E−06	
vfr	5	Transcriptional regulator	1.04E−05	
PA4133	6	Cytochrome *c* oxidase subunit (cbb_3 type)	4.17E−05	
PA4021	6	Probable transcriptional regulator	2.13E−04	
PA4873	5	Probable heat shock protein	2.42E−04	
pqqD	3	Pyrroloquinoline quinone biosynthesis protein D	2.58E−04	
exbB1	4	Transport protein ExbB	2.89E−04	
PA2802	4	Probable transcriptional regulator	2.89E−04	
ureD	4	Urease accessory protein	5.19E−04	
pqqF	6	Pyrroloquinoline quinone biosynthesis protein F	5.64E−04	
hitB	5	Iron (III) transport system permease	5.83E−04	
PA0181	4	Probable transcriptional regulator	7.55E−04	
PA4180	5	Probable acetolactate synthase large subunit	7.82E−04	
PA3900	4	Probable transmembrane sensor	8.20E−04	
PA0041	13	Probable hemagglutinin	8.20E−04	
PA2511	4	Probable transcriptional regulator	9.81E−04	

[a]Genes within the Pf4 phage encoded region identified by this test were excluded from this table. Genes encoding hypothetical proteins identified by this test are listed in Table S2. Genes *migA* and *algP* were identified as significant but were also identified in the control population evolved in the absence of colistin. Hence, those genes are considered to be involved in adaptation to the bioreactor rather than the drug.
[b]LPS, lipopolysaccharide.

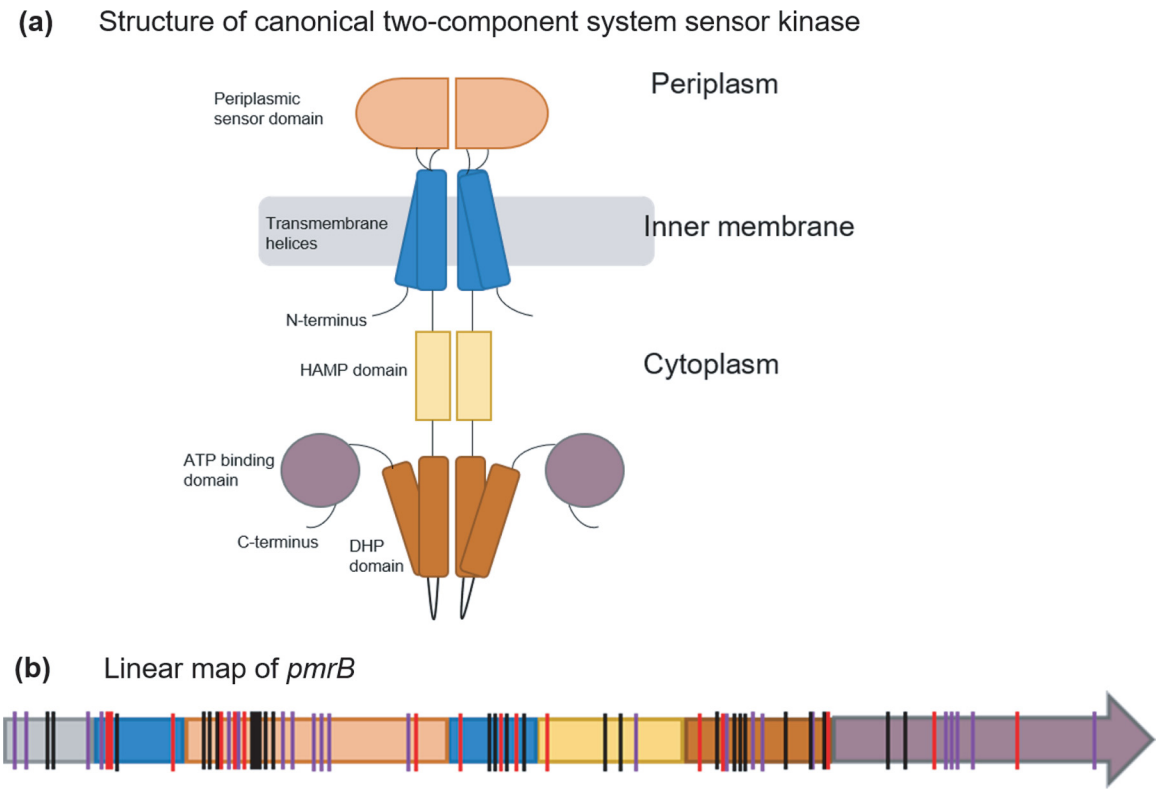

FIG 5 (a and b) Structural representation of a canonical two-component system sensor kinase dimer (adapted from reference 51 with permission of the publisher) (a) and linear map of *pmrB* showing positions of identified mutations (b). The color scheme for domains used in panel a is maintained in panel b. (b) Mutations identified in *pmrB* in this study as well as previous works have been indicated by vertical lines on the *pmrB* gene. Red lines represent mutations identified in this study. Black lines represent mutations observed in other evolution experiments (12, 13, 28, 32), and purple lines represent mutations identified in colistin-resistant clinical *P. aeruginosa* isolates (10–12, 27, 33, 34, 52). HAMP, histidine kinases, adenylate cyclases, methyltransferases, and phosphodiesterases; DHP, dimerization and histidine phosphotransfer. Domain assignments in the PmrB protein are based on the predicted domain structure of PmrB by Moskowitz et al. (27). Details of the types of mutations observed in each domain of PmrB in this study can be found in File S1.

phylogenetic trees (Fig. 3) to visualize the diversity and distribution of mutations among the endpoint isolates. The adaptive trajectories of these mutations are shown in Fig. S3 and S4. Table 1 provides a list of candidates identified as putative players in colistin resistance among endpoint isolates, and Fig. S5 shows their cellular localization.

The number and variety of mutations observed in *pmrB* suggest that only modest changes in PmrB function are required for increased colistin resistance. PmrB is the sensor kinase of a two-component system, PmrAB, and is involved in sensing cationic antimicrobial peptides (CAPs) (31). It was noteworthy that during the course of adaptation to colistin, 19 independent mutations were detected in *pmrB* using a 5% frequency cutoff for mutation detection. Eighteen of these mutations were single nucleotide polymorphisms (SNPs) that led to amino acid modifications affecting all the domains within this protein, while one mutation was a 3-bp deletion leading to the loss of amino acid 47 in PmrB. Out of the 19 mutations, three (L167P, L170P, and F408L) were observed independently in duplicate experiments, and thus, 16 unique mutations were identified in *pmrB*.

Figure 5 shows the putative relationship of PmrB based on canonical sensor kinases of two-component systems. From the positions of mutations shown in red in Fig. 5b, it is clear that every domain of PmrB was a potential target for adaptive mutations in this study. Also identified in this figure are adaptive mutations identified previously in clinical and lab-adapted *P. aeruginosa* strains (indicated in purple and black) highlighting the plasticity of the gene encoding this protein to acquire mutations. The propensity of *pmrB* to accumulate mutations at many locations suggests that modest changes

TABLE 3 Comparison of constructed *pmrB* mutants and bioreactor-derived endpoint isolates having the same *pmrB* mutation

Wild type or mutation	Colistin MIC (μg/ml) of:		Frequency of mutation at the end of adaptation (replicates 1 and 2) (%)	No. of additional mutations in endpoint isolates having this mutation
	Constructed mutant	Endpoint isolates with this mutation[a]		
WT	1 or 2			
L17P	2	>128	46	Not determined[b]
L18P	8	16–128	10	53–62
D47G	8	16	4.3	Not determined[b]
L243R	4	16–32	5.1	60–74
F408L	4	8–64	3.6 and 22.8	56–68

[a]Ranges are MICs for different endpoint isolates with this mutation.
[b]Whole-genome sequencing was not performed for these endpoint isolates.

in PmrB function are sufficient to alter the expression of genes in the regulon of this two-component system sensor kinase and confer resistance.

Introduction of *pmrB* mutations in a wild-type PAO1 background indicates that other mutations are needed to explain the high levels of resistance. Multiple adaptive mutations identified in colistin-resistant endpoint isolates suggested the possibility of clonal interference, where multiple beneficial mutations in the population were competing with one another for success in the population (20). Since the role of PmrB in CAP resistance is known, we wanted to determine if specific changes in PmrB were sufficient to explain the very high MICs of some of the bioreactor-derived endpoint isolates as well as clinical isolates from previous studies (27). Allelic replacement was used to identify the role of individual *pmrB* mutations in resistance by creating point mutations in *pmrB* within a wild-type PAO1 background. Five such constructs were made, each containing one *pmrB* mutation identified in the colistin resistance-evolved PAO1 populations from this work (L17P, L18P, D47G, L243R, and F408L). These constructs and their respective bioreactor-derived endpoint isolates were tested to compare colistin MICs (Table 3). Three *pmrB* mutations were observed in endpoint isolates that had been selected for whole-genome sequencing, L18P, L243R, and F408L. Sanger sequencing was used to identify the sequence of *pmrB* in a few other endpoint isolates and 2 isolates, labeled as 11 and 17, were selected that had the D47G and L17P mutations in PmrB, respectively. There is no information regarding other mutations in these isolates since the whole genomes of these isolates were not sequenced.

From Table 3, it is evident that different mutations within *pmrB* contribute to different levels of colistin resistance. While a mutation constructed in the transmembrane domain of PmrB, L18P, imparted complete resistance to colistin (MIC, 8 μg/ml), the adjacent mutation L17P did not (MIC, 2 μg/ml). The mutation L18P first appeared on day 18 of adaptation (replicate 1), while L17P was seen only during the final day of adaptation when the population was growing in the presence of 16 mg/liter colistin (Fig. S4). While early mutations during adaptation are often the most beneficial, additional mutations conferring typically smaller advantages can arise later (37, 38). The appearance of L18P earlier during adaptation provided resistance to members of a population that was still evolving, suggesting that it might be a primary mutation. The mutation L17P, which appeared later when the population was already growing at a high drug concentration (16 μg/ml), was not an early primary mutation but may have played a role in enhancing the level of resistance in a specific genomic background that had achieved initial success (12). Other point mutations in the periplasmic domain (D47G), dimerization and phosphotransferase (L243R), and in the C-terminal ATP binding domains (F408L) all imparted resistance to colistin with the highest MIC at 8 μg/ml, while their corresponding bioreactor-derived endpoint isolates consistently had acquired higher levels of resistance. These data provide strong evidence for the role of epistasis in high resistance of the bioreactor-derived endpoint isolates.

PAO1 incurs a fitness cost as a trade-off to acquiring colistin nonsusceptibility. Growth characteristics of the constructed mutants and bioreactor-derived endpoint

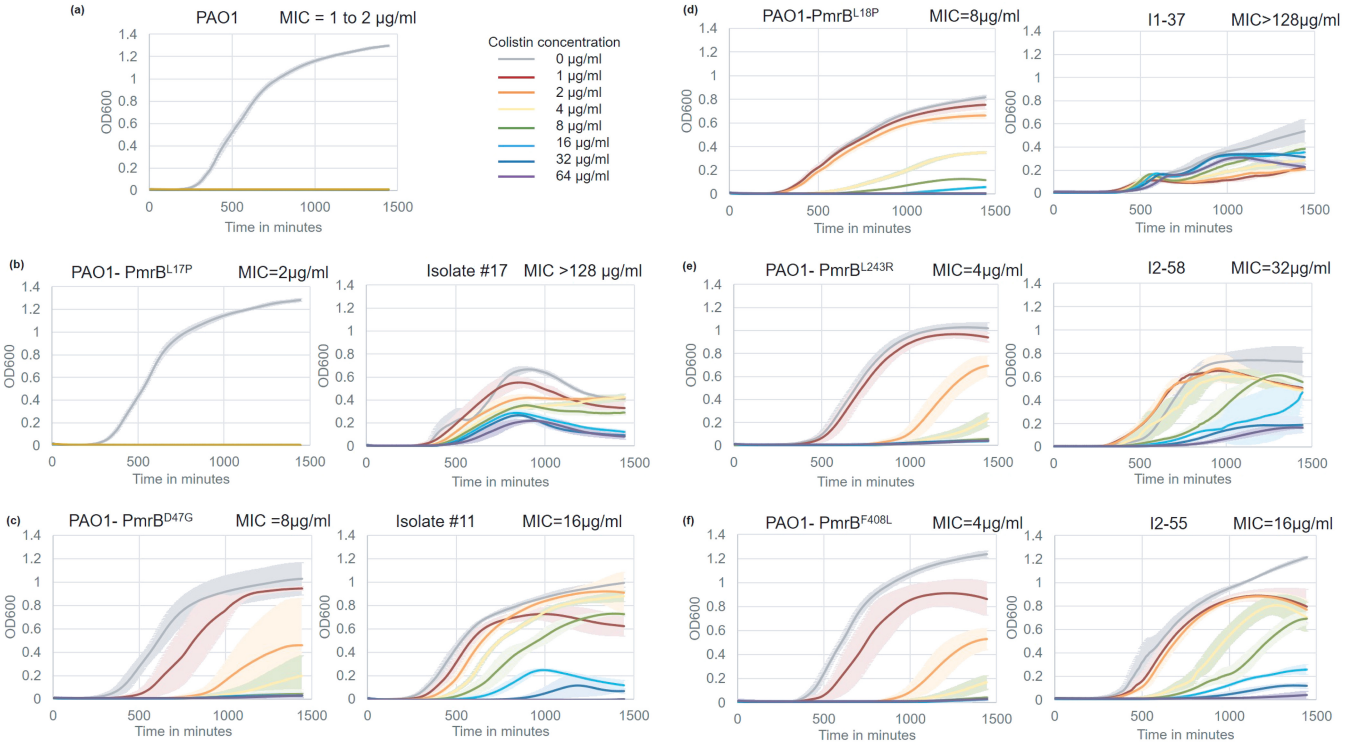

FIG 6 Growth characteristics of PAO1 ancestor, constructed point mutants, and bioreactor-adapted endpoint isolates. Each panel (except panel a) represents the constructed mutant on the left and the bioreactor-adapted endpoint isolate carrying the same *pmrB* mutation on the right. All growth assays were conducted at colistin concentrations ranging from 0 to 64 μg/ml. Error bars represent the standard deviation of the results from three biological replicates. The MICs of all these strains, measured by broth microdilution, are on the top-right corner of each graph.

isolates possessing the same mutations shed light on the fitness of the mutants in the presence and absence of colistin (Fig. 6). The growth of the ancestor PAO1 served as the reference (Fig. 6a). It was clear from our data that higher levels of colistin resistance that were associated with hypermutation led to reduced fitness in the isolates.

pmrB point mutants constructed in a wild-type background could resist up to 8 μg/ml colistin without undergoing a severe growth defect in the absence of the drug. In comparison, bioreactor isolates with the same *pmrB* mutations that had higher levels of resistance had decreased fitness in the absence of the drug. Bioreactor isolate I1-37 (doubling time, 397 $\pm$ 90 min; MIC, $>$128 μg/ml) grew more than two times slower than did the point mutant PmrB^{L18P} (doubling time, 165 $\pm$ 5 min; MIC, 8 μg/ml) in the absence of colistin (Fig. 6d). Isolate I1-37, which had 59 mutations in addition to PmrB^{L18P}, also had an increased lag time (longer by approximately 125 min) and lower overall yield but had the ability to survive in the presence of higher levels of colistin. Similarly, bioreactor isolate I2-55 (MIC, 16 μg/ml) had a 2-fold decrease in growth rate compared to that of the point mutant PmrB^{F408L} (MIC, 4 μg/ml) (Fig. 6f). However, it was capable of achieving nearly the same final cell density as PmrB^{F408L} and the ancestor strain (Fig. 6a), suggesting that higher levels of resistance, as seen in I1-37, were associated with greater fitness defects. Although PmrB^{L17P} alone offered no adaptive advantage (Fig. 6a), bioreactor-derived isolate no. 17 that had a very high colistin MIC also had a severe growth defect.

The balance between acquisition of resistance and the associated fitness costs was further supported by allelic replacements to produce PmrB^{D47G} and PmrB^{L243R} in the wild-type PAO1 background. These adaptive mutants were only modestly less fit in terms of growth rate and yield (Fig. 6c, e, and f) under nonselective conditions but were able to grow better than wild-type PAO1 in the presence of colistin, which is also true for their corresponding bioreactor-derived endpoint isolates.

Our data suggest that while *P. aeruginosa* acquires myriad mutations to resist colistin, the accumulation of these mutations comes at a fitness cost to the cells, and higher levels of resistance are usually accompanied by a more severe growth phenotype in hypermutators. The advantage of mutation supply in a hypermutator is offset by the fitness defect of the evolved isolates. In spite of the fitness cost, resistance to this drug of last resort in *P. aeruginosa* clinical isolates has been observed (39–41), which underscores the importance of understanding the mechanism of colistin resistance for the design of new strategies that can circumvent this problem.

DISCUSSION

The development of a hypermutator phenotype is a common occurrence in clinical settings and can lead to rapid adaptation to antibiotics (2, 14). Hypermutators increase the mutation supply within the evolving population, allowing natural selection to act upon a more genetically diverse population, thereby increasing the probability that a successful, e.g., a more antibiotic-resistant variant, can be found (18). The increased mutation load, however, comes with a cost to overall fitness as nonadaptive or hitchhiker mutations accumulate within the genomes of the hypermutators (15, 26). As a random mutation is much more likely to be deleterious, the accumulation of these random mutations brings consequences to fitness, especially when the selection pressure of the antibiotic is removed. For example, endpoint isolates with increased MICs to colistin had substantially decreased growth rates in the absence of colistin (Fig. 6). While an increased mutation rate may be a poor long-term evolutionary path for organisms like *P. aeruginosa*, the short-term benefit is clear. Interestingly, in our bioreactor environments that strongly favor the formation of biofilms, susceptible and nonhypermutator cells persisted despite the vessel containing >2 μg/ml colistin for 2 weeks in the case of replicate 1 (Fig. 2). A similar observation was made in a recent study where mixed biofilms containing a combination of susceptible and drug-resistant PAO1 cells offered protection to the susceptible cells upon antibiotic exposure (42). We speculate that the biofilms insulate these weaker variants (see File S1) and can act as a reservoir for reestablishing a more fit population if the colistin were withdrawn. In an infected individual, such as a cystic fibrosis patient, such a reservoir could suggest that when the antibiotic is switched, the more fit *P. aeruginosa* strains can reemerge, and conversely, that colistin-resistant variants could now be a reservoir for reestablishing the colistin-resistant population if the patient returned to colistin therapy. Thus, the combination of hypermutation and strong biofilms can lead to the persistent and difficult-to-treat infections that are a hallmark of *P. aeruginosa*.

It has been suggested that because of the large number of hitchhiker mutations that succeed in the population under conditions of selection, the signature of selection in the genome is very weak, making it difficult to distinguish driver alleles from passenger mutations (15). We show that it is possible to identify the signature of selection in an adapting hypermutator population using a combination of genomic and statistical approaches. Quantitative experimental evolution provides a ready means to construct the genomic data needed for analysis (13, 16, 19–21). We propose a hierarchy of analyses beginning with Fisher's exact test of both endpoint isolates and longitudinal metagenomic data to build and rank a list of candidate genes that are putatively involved in resistance. This method has proven useful in the identification of adaptive mutations in previous studies involving hypermutation and weak selection (16, 19). We also construct phylogenetic trees of the endpoint isolates that provide further genetic and evolutionary structure to the candidate list. Furthermore, we use the information about the frequencies of these mutations in the daily populations to build parsimonious evolutionary trajectories for the most important drivers for colistin resistance, and taken together, these trajectories illustrate what we term the "adaptive genome" of *P. aeruginosa* to the selection environment (Fig. 7).

Using genetics and phenotypic analysis of growth rates, we establish that epistatic interactions between multiple mutations in the bioreactor-derived hypermutator endpoint isolates are most likely responsible for the observed higher levels of colistin

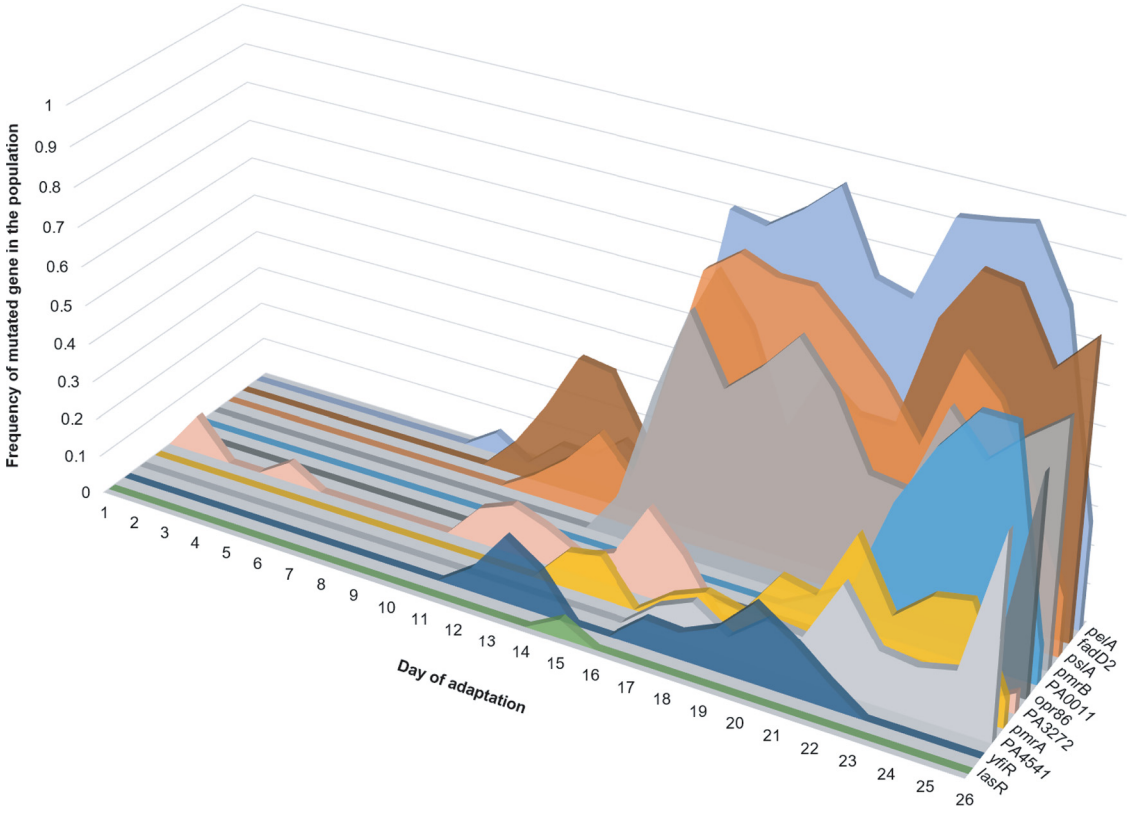

FIG 7 Adaptive genome of a *P. aeruginosa* population (replicate 1) evolving to colistin. Most adaptive genes had multiple mutations within them during the course of adaptation. On a given day, the sum of frequencies of the different alleles within a gene was calculated and plotted on the *y* axis. The *x* axis represents the day of adaptation, and the *z* axis represents each gene. Genes represented here include putative candidates listed in Table 1 and selected candidates from Table 2 (selection based on their appearance in other polymyxin resistance studies).

resistance which comes at a fitness cost to the cells in terms of reduced growth rate and overall yield (Fig. 6). Such epistatic interactions between multiple alleles imply that high levels of colistin resistance can be acquired via multiple adaptive routes which in turn result in the formation of a rugged fitness landscape with many local peaks, each representing a local optimum. Hypermutation provides an effective means for the cells to access this landscape during selection.

In summary, this work sheds light on multiple features of the evolvability of *P. aeruginosa* to the drug of last resort, colistin. While the complexities of hypermutation have hindered progress, it has become increasingly clear that next-generation sequencing and experimental evolution provide a path forward to the study of this clinically and conceptually important evolutionary mechanism for adaptation (13, 16, 43). The methodological approaches within this work show that hypermutation can be studied successfully to produce a broad understanding of adaptive evolution in established and future emerging pathogens.

MATERIALS AND METHODS

Bacterial strains, plasmids, and growth conditions. *P. aeruginosa* PAO1 was obtained from American Type Culture Collection (ATCC 15692). Plasmid pEX18Gm was kindly provided by Herbert Schweizer. PAO1 was routinely grown in lysogeny broth (LB; 10 g/liter tryptone, 5 g/liter yeast extract, 10 g/liter sodium chloride) or on LB plus 15 g/liter Bacto agar. The growth medium for adaptation of PAO1 to colistin was LBHI (80% LB plus 20% brain heart infusion [BHI] medium) supplemented with 2 mM magnesium sulfate and an appropriate concentration of colistin. Colistin stock solution was made by dissolving colistin sulfate (DOT Scientific Inc., MI, USA) in water, followed by filter sterilization using a 0.22-μm filter. Cation-adjusted Mueller-Hinton broth (CA-MHB) was used for MIC testing and growth curves. Gentamicin at 20 μg/ml was used for maintenance of pEX18Gm in *Escherichia coli*, and 60 μg/ml was used for growing PAO1 transformed with the pEX18-*pmrB* plasmid. The strains and plasmids used in this study are listed in Table 4.

TABLE 4 Bacterial strains, plasmids, and primers used in this study

Strain or plasmid	Characteristics or sequence[a]	Reference, source, or template
Strains		
PAO1	*Pseudomonas aeruginosa* ancestor	ATCC 15692
NEB 5-alpha	*Escherichia coli* DH5α derivative	New England BioLabs C2987I
PAO1-PmrB^{F408L}	Point mutant PAO1 *pmrB*$^{1222T\rightarrow C}$ encoding PmrB^{F408L}	This study
PAO1-PmrB^{D47G}	Point mutant PAO1 *pmrB*$^{140A\rightarrow G}$ encoding PmrB^{D47G}	This study
PAO1-PmrB^{L243R}	Point mutant PAO1 *pmrB*$^{728T\rightarrow G}$ encoding PmrB^{L243R}	This study
PAO1-PmrB^{L18P}	Point mutant PAO1 *pmrB*$^{53T\rightarrow C}$ encoding PmrB^{L18P}	This study
PAO1-PmrB^{L17P}	Point mutant PAO1 *pmrB*$^{50T\rightarrow C}$ encoding PmrB^{L17P}	This study
Plasmids		
pEX18Gm	Gm^r; *oriT*$^+$ *sacB*$^+$, gene replacement vector with MCS from pUC18	55
pEX18Gm-*pmrB*$^{1222T\rightarrow C}$	*pmrB*$^{1222T\rightarrow C}$ allelic exchange vector for mutant encoding PmrB^{F408L}	This study
pEX18Gm-*pmrB*$^{140A\rightarrow G}$	*pmrB*$^{140A\rightarrow G}$ allelic exchange vector for mutant encoding PmrB^{D47G}	This study
pEX18Gm-*pmrB*$^{728T\rightarrow G}$	*pmrB*$^{728T\rightarrow G}$ allelic exchange vector for mutant encoding PmrB^{L243R}	This study
pEX18Gm-*pmrB*$^{53T\rightarrow C}$	*pmrB*$^{53T\rightarrow C}$ allelic exchange vector for mutant encoding PmrB^{L18P}	This study
pEX18Gm-*pmrB*$^{50T\rightarrow C}$	*pmrB*$^{50T\rightarrow C}$ allelic exchange vector for mutant encoding PmrB^{L17P}	This study
Primers by function		
Cloning *pmrB*^{F408L} into pEX18Gm		
F408L-500F	ctgcaaggcgattaagttggCTCATCGACGAACTCAACCT	I2-55
F408L-500R	gattacgaattcgagctcggCTCCTCGATCTTGCGATTCA	
pEX-F408L-500F	TGAATCGCAAGATCGAGGAGccgagctcgaattcgtaatc	pEX18Gm
pEX-F408L-500R	AGGTTGAGTTCGTCGATGAGccaacttaatcgccttgcag	
Cloning *pmrB*^{D47G} into pEX18Gm		
pmrB-D47G-fwd	ctgcaaggcgattaagttggTGACCAAGCCCTTCGATCTCG	Colony no. 11
pmrB-D47G-rev	gattacgaattcgagctcggGCGGATCTCCAGCGGTACCG	
pEX-D47G-fwd	CGGTACCGCTGGAGATCCGCccgagctcgaattcgtaatc	pEX18Gm
pEX-D47G-rev	GAGATCGAAGGGCTTGGTCAccaacttaatcgccttgcag	
Cloning *pmrB*^{L243R} into pEX18Gm		
pmrB-L243R-fwd	ctgcaaggcgattaagttggGACCTTGCCACCGAAGACCA	I2-58
pmrB-L243R-rev	gattacgaattcgagctcggGTAGAAGCGGGTGAAGATCG	
pEX-L243R-fwd	CGATCTTCACCCGCTTCTACccgagctcgaattcgtaatc	pEX18Gm
pEX-L243R-rev	TGGTCTTCGGTGGCAAGGTCccaacttaatcgccttgcag	
Cloning *pmrB*^{L18P} into pEX18Gm		
L18P-450F	tgtgctgcaaggcgattaagCCGACGACTACCTGACCAAG	I1-58
L18P-450R	ggtacccggggatcctctagGTAGAACAGCAGCAGGTTCA	
pEX-L18P-450F	TGAACCTGCTGCTGTTCTACctagaggatccccgggtacc	pEX18Gm
pEX-L18P-450R	CTTGGTCAGGTAGTCGTCGGcttaatcgccttgcagcaca	
Cloning *pmrB*^{L17P} into pEX18Gm		
L18P-450F	tgtgctgcaaggcgattaagCCGACGACTACCTGACCAAG	Colony no. 17
L18P-450R	ggtacccggggatcctctagGTAGAACAGCAGCAGGTTCA	
pEX-L18P-450F	TGAACCTGCTGCTGTTCTACctagaggatccccgggtacc	pEX18Gm
pEX-L18P-450R	CTTGGTCAGGTAGTCGTCGGcttaatcgccttgcagcaca	

[a]Gm^r, gentamicin resistance; MCS, multiple cloning site. For each primer, the uppercase and lowercase letters distinguish the tails from the priming regions.

Evolution of PAO1 to colistin resistance. PAO1 was evolved to colistin resistance in a modified turbidostat as described by Mehta et al. (24). In duplicate experiments, a 300-ml PAO1 culture was established in the bioreactor vessel by using a single colony as an inoculum. The culture was maintained in mid-exponential-growth phase using respiratory CO_2 as a proxy for turbidity to control the medium flow. After 12 h of growth, the first subinhibitory dose of colistin was added to the vessel (0.5 μg/ml). After that, the culture was monitored, and the drug concentration was empirically increased. Details of the process are provided by Mehta et al. (24). PAO1 was able to grow at 18 μg/ml colistin after 26 days of evolution during replicate 1 and at 16 μg/ml colistin after 17 days of evolution during replicate 2. The control experiment was performed in an identical manner without the addition of colistin (no-drug control). The control population was grown for 14 days.

Isolation and characterization of endpoint isolates. The final resistant population of PAO1 was serially diluted and spread on nonselective medium (LBHI plus 2 mM magnesium sulfate) to isolate individual members of the population. Each colony was called an endpoint isolate. Eighty-eight endpoint isolates were selected from replicate 1 and 82 isolates from replicate 2 for further phenotypic characterization. Morphological characteristics were recorded for each isolate, which included colony size, shape, color, consistency, and appearance when grown in a nonselective liquid medium (File S1). The MIC of colistin was tested using a preliminary broth microdilution assay. A colistin gradient (0 to 128 μg/ml) was set up in a 96-well polypropylene plate containing 100 μl CA-MHB per well. One microliter of an overnight culture (grown in LBHI plus 2 mM magnesium sulfate) for each isolate was used as an inoculum. Plates were incubated at 37°C, and visible growth was recorded after 20 to 24 h. The lowest colistin concentration showing absence of growth was the MIC. The MICs of other antibiotics were also

tested for determining cross-sensitivity/cross-resistance to other drugs. Agar dilution MIC assays were performed for this in 150-mm petri dishes containing CA-MH agar with appropriate drug concentration. A 96-pin applicator was used to spot the overnight culture of each isolate on the agar plates. MICs were recorded after 20 to 24 h of incubation at 37°C. Based on the different phenotypic traits, 15 endpoint isolates from replicate 1 and 14 isolates from replicate 2 were selected for whole-genome sequencing and mutation identification. Cross-sensitivities to other antibiotics were observed in some endpoint isolates, but a correlation of the cross-sensitivity to colistin resistance could not be established; hence, this phenotype was not pursued further.

MIC assay. Broth microdilution MIC tests in biological triplicate were performed for the 29 endpoint isolates selected for whole-genome sequencing using 96-well polypropylene plates. Each well was filled with 100 μl CA-MHB and an appropriate concentration of colistin (0 to 128 μg/ml colistin in 2-fold increments). Overnight cultures for endpoint isolates were grown in biological triplicates in LBHI plus 2 mM magnesium sulfate. The optical densities of the cultures were adjusted to 0.05, and 5 μl of this OD-adjusted culture was used to inoculate each well of the plates. Growth was checked visually after 20 to 24 h of incubation at 37°C, and MICs were recorded. Identical MIC tests using LBHI plus 2 mM $MgSO_4$ instead of CA-MHB were also performed, and similar MICs were observed (within 2-fold difference in MIC values).

Whole-genome sequencing and analysis. DNA isolation and whole-genome sequencing were performed as described by Mehta et al. (24). Samples from replicate 1 of adaptation were sequenced at the U.S. Army Edgewood Chemical Biological Center (ECBC, MD, USA) as 100-bp paired-end reads, and samples from replicate 2 and daily populations of the no-drug control were sequenced by a commercial facility (Genewiz, NJ, USA) as 150-bp paired-end reads. Read trimming of raw Fastq reads was performed using Sickle (44). Trimmed reads were analyzed using breseq version 0.30.1 and 0.33.2 (45) to identify genetic variations between ancestor and adaptive populations as well as endpoint isolates. The genome sequence of the ancestor was obtained from the NCBI (GenBank accession no. AE004091). The ancestor colony used to inoculate the bioreactor during each replicate was resequenced, and the APPLY function in breseq was used to incorporate any differences in the genome of the resequenced ancestor strain into the NCBI reference genome before using it to identify mutations in the evolved strains. The consensus mode was used for the identification of mutations in the endpoint isolates. The polymorphism mode in breseq was used for the analysis of daily metagenomic populations from the bioreactor using the following command: -p –polymorphism-reject-surrounding-homopolymer-length 5 –polymorphism-reject-indel-homopolymer-length 0 –polymorphism-minimum-coverage-each-strand 6 –polymorphism-frequency-cutoff 0.02. To filter low-quality mutations from the daily populations under analysis, two additional quality filtering steps were added after the breseq analysis of each daily sample. It was observed that the number of false calls increased substantially for low-frequency mutations. Thus, mutations in the daily populations that fell below a threshold of 5% frequency in the population were filtered out. Second, it was found that mutations had been called in several reads that had low mapping quality (MQ) scores. Mutations in regions that contained three or more reads having an MQ score less than 100 were also filtered out. Also, reads were manually examined, and mutation calls which were characterized by 3 or more mutations clustered within a read at low frequencies and whose occurrence was not consistent with adaptation or hitchhiking were eliminated from further analysis. Data Set S1 contains a list of all mutations and their frequencies on each day of evolution during replicates 1 and 2 as well as in the control population.

Construction of phylogenetic trees. The breseq output for each endpoint isolate contained a list of mutations in the genome of the endpoint isolate. The APPLY function in breseq was used to apply the mutations in the endpoint isolate onto the PAO1 reference genome to create a genome sequence for each endpoint isolate. Next, the genome of the reference strain was manually aligned with that of all the endpoint isolates using the software MEGA7 (46). Phylogenetic trees were constructed for both replicates using the maximum parsimony algorithm based on reference 47 as implemented in MEGA7. These trees were then visualized using the Dendroscope3 software (48).

Fisher's exact test. To perform Fisher's exact test on endpoint isolates, a list of the total number of mutations occurring in a gene was compiled from the breseq output file. Gene lengths were obtained from the *Pseudomonas* Genome Database (49) by mapping the gene name to the gene length. A few genes without matches were manually given gene lengths. With the compiled list containing the number of mutations per gene, the length of the gene, the total number of mutations in all endpoint isolates or populations, and the total length of the PAO1 genome, Fisher's exact test was performed using the fisher.test function in R with a two-sided alternative hypothesis and a significance threshold of 0.001.

Construction of point mutations in PAO1 *pmrB*. Point mutants in PAO1 were constructed using the protocol described by Huang and Wilks (50), with minor modifications. pEX18Gm was used instead of pEX18Tc. Allelic exchange vectors (Table 4) were made using the Gibson Assembly master mix (New England BioLabs) with primers listed in Table 4. Mutant *pmrB* alleles were amplified from the respective bioreactor-derived endpoint isolate containing the mutation. Electroporation of the constructed plasmid into PAO1 was done at room temperature using a 2-mm-gap electroporation cuvette at 2.2 kV, as described previously (50). Electroporated cells were spread on BHI plus 60 μg/ml gentamicin (Gm) plates and incubated at 37°C for 2 to 3 days. Gm-resistant colonies were colony purified on BHI plus Gm60 plates, and single colonies were streaked on no-salt LB (NSLB) plus 15% sucrose plates and incubated at 30°C for sucrose counterselection. Sucrose-resistant colonies were tested for Gm sensitivity, and for colonies that were Gm sensitive and sucrose resistant, the *pmrB* gene was amplified and sequenced using Sanger sequencing to determine the presence of the point mutation.

Growth curves. Overnight cultures were prepared in LB broth in biological triplicates. Optical densities were measured and normalized to 0.05. Ninety-six-well polypropylene plates were used for growth curves. Each well was filled with 100 μl CA-MHB, and a colistin gradient was set up for concentrations ranging from 0 to 64 μg/ml. Each well was inoculated with 1 μl of the OD-normalized culture, and growth was measured in each well using a BioTek Epoch2 microplate reader at 37°C for 24 h, with optical density being measured at 5-min intervals. The OD of plain CA-MHB (blank reading) was subtracted from the OD of the samples at every time point. Exponential smoothing was applied to each data series to account for the noise in the OD measurements due to clumping and biofilm formation in the wells. The final graph of OD versus time was plotted using the average of 3 biological replicates with standard deviations. Doubling times were calculated in the OD_{600} interval of 0.2 to 0.4.

Data availability. The whole-genome sequencing data generated during this study were submitted to the Sequence Read Archive (SRA) database under BioProject accession number PRJNA486960.

SUPPLEMENTAL MATERIAL

Supplemental material for this article may be found at https://doi.org/10.1128/AAC.00744-19.

SUPPLEMENTAL FILE 1, PDF file, 1.2 MB.

SUPPLEMENTAL FILE 2, XLSX file, 0.6 MB.

ACKNOWLEDGMENTS

We are thankful to Luay Nakhleh for his assistance with computational analysis and resources. We are thankful to Herbert Schweizer for kindly providing plasmids for genetically modifying *P. aeruginosa*. We appreciate the advice provided by Weiliang Huang and Angela Wilks for isolation and identification of mutant *P. aeruginosa* candidates following allelic replacement. We are grateful to Jeff Barrick for assistance with analysis of metagenomic population data using breseq.

This work is supported by funds from the Defense Threat Reduction Agency (grant HDTRA1-15-1-0069) to Y.S., a National Institutes of Health fellowship (grant F31GM108402NIAID) to K.B., and the National Science Foundation (grant DMS-1547433) to Luay Nakhleh (principal investigator [PI]) and R.A.L.E. (trainee).

The content of the information in this paper does not necessarily reflect the position or the policy of the federal government, and no official endorsement should be inferred.

We declare no competing interests.

Y.S. conceived of the idea. H.H.M., A.G.P., and K.B. conducted the bioreactor adaptation experiments. M.K. and H.S.G. conducted whole-genome sequencing for replicate 1 of this project. H.H.M. was involved in analyzing the whole-genome sequencing (WGS) data and in mutation identification. R.A.L.E. performed the phylogenetic and statistical analyses. H.H.M. performed the phenotypic characterization and allelic replacements. H.H.M. and Y.S. wrote the manuscript. All authors provided critical feedback and contributed to the manuscript.

REFERENCES

1. Swings T, Van Den Bergh B, Wuyts S, Oeyen E, Voordeckers K, Verstrepen KJ, Fauvart M, Verstraeten N, Michiels J. 2017. Adaptive tuning of mutation rates allows fast response to lethal stress in *Escherichia coli*. Elife 6:e22939. https://doi.org/10.7554/eLife.22939.
2. Hall LMC, Henderson-Begg SK. 2006. Hypermutable bacteria isolated from humans–a critical analysis. Microbiology 152:2505–2514. https://doi.org/10.1099/mic.0.29079-0.
3. Sundin GW, Weigand MR. 2007. The microbiology of mutability. FEMS Microbiol Lett 277:11–20. https://doi.org/10.1111/j.1574-6968.2007.00901.x.
4. Ciofu O, Riis B, Pressler T, Poulsen HE, Høiby N. 2005. Occurrence of hypermutable *Pseudomonas aeruginosa* in cystic fibrosis patients is associated with the oxidative stress caused by chronic lung inflammation. Antimicrob Agents Chemother 49:2276–2282. https://doi.org/10.1128/AAC.49.6.2276-2282.2005.
5. Waine DJ, Honeybourne D, Smith EG, Whitehouse JL, Dowson CG. 2008. Association between hypermutator phenotype, clinical variables, mucoid phenotype, and antimicrobial resistance in *Pseudomonas aeruginosa*. J Clin Microbiol 46:3491–3493. https://doi.org/10.1128/JCM.00357-08.
6. Oliver A, Canton R, Campo P, Baquero F, Blazquez J. 2000. High frequency of hypermutable *Pseudomonas aeruginosa* in cystic fibrosis lung infection. Science 288:1251–1253. https://doi.org/10.1126/science.288.5469.1251.
7. Mulcahy LR, Isabella VM, Lewis K. 2014. *Pseudomonas aeruginosa* biofilms in disease. Microb Ecol 68:1–12. https://doi.org/10.1007/s00248-013-0297-x.
8. Flynn KM, Dowell G, Johnson TM, Koestler BJ, Waters CM, Cooper VS. 2016. Evolution of ecological diversity in biofilms of *Pseudomonas aeruginosa* by altered cyclic diguanylate signaling. J Bacteriol 198:2608–2618. https://doi.org/10.1128/JB.00048-16.
9. Rumbaugh KP. 2014. Genomic complexity and plasticity ensure *Pseudomonas* success. FEMS Microbiol Lett 356:141–143. https://doi.org/10.1111/1574-6968.12517.
10. Lee JY, Na IY, Park YK, Ko KS. 2014. Genomic variations between colistin-susceptible and -resistant *Pseudomonas aeruginosa* clinical isolates and

their effects on colistin resistance. J Antimicrob Chemother 69:1248–1256. https://doi.org/10.1093/jac/dkt531.
11. Abraham N, Kwon DH. 2009. A single amino acid substitution in PmrB is associated with polymyxin B resistance in clinical isolate of *Pseudomonas aeruginosa*. FEMS Microbiol Lett 298:249–254. https://doi.org/10.1111/j.1574-6968.2009.01720.x.
12. Jochumsen N, Marvig RL, Damkiær S, Jensen RL, Paulander W, Molin S, Jelsbak L, Folkesson A. 2016. The evolution of antimicrobial peptide resistance in *Pseudomonas aeruginosa* is shaped by strong epistatic interactions. Nat Commun 7:13002. https://doi.org/10.1038/ncomms13002.
13. Dößelmann B, Willmann M, Steglich M, Bunk B, Nubel U, Peter S, Neher RA. 2017. Rapid and consistent evolution of colistin resistance in extensively drug-resistant *Pseudomonas aeruginosa* during morbidostat culture. Antimicrob Agents Chemother 61:e00043-17. https://doi.org/10.1128/AAC.00043-17.
14. Denamur E, Matic I. 2006. Evolution of mutation rates in bacteria. Mol Microbiol 60:820–827. https://doi.org/10.1111/j.1365-2958.2006.05150.x.
15. Couce A, Caudwell LV, Feinauer C, Hindré T, Feugeas J, Weigt M, Lenski RE, Schneider D, Tenaillon O. 2017. Mutator genomes decay, despite sustained fitness gains, in a long-term experiment with bacteria. Proc Natl Acad Sci 114:9026–9035. https://doi.org/10.1073/pnas.1705887114.
16. Hammerstrom TG, Beabout K, Clements TP, Saxer G, Shamoo Y. 2015. *Acinetobacter baumannii* repeatedly evolves a hypermutator phenotype in response to tigecycline that effectively surveys evolutionary trajectories to resistance. PLoS One 10:e0140489. https://doi.org/10.1371/journal.pone.0140489.
17. Dettman JR, Sztepanacz JL, Kassen R. 2016. The properties of spontaneous mutations in the opportunistic pathogen *Pseudomonas aeruginosa*. BMC Genomics 17:27. https://doi.org/10.1186/s12864-015-2244-3.
18. Tenaillon O, Taddei F, Radman M, Matic I. 2001. Second-order selection in bacterial evolution: selection acting on mutation and recombination rates in the course of adaptation. Res Microbiol 152:11–16. https://doi.org/10.1016/S0923-2508(00)01163-3.
19. Saxer G, Krepps MD, Merkley ED, Ansong C, Kaiser BLD, Valovska M-T, Ristic N, Yeh PT, Prakash VP, Leiser OP, Nakhleh L, Gibbons HS, Kreuzer HW, Shamoo Y. 2014. Mutations in global regulators lead to metabolic selection during adaptation to complex environments. PLoS Genet 10:e1004872. https://doi.org/10.1371/journal.pgen.1004872.
20. Cooper VS. 2018. Experimental evolution as a high-throughput screen for genetic adaptations. mSphere 3:e00121-18. https://doi.org/10.1128/mSphere.00121-18.
21. Miller C, Kong J, Tran TT, Arias CA, Saxer G, Shamoo Y. 2013. Adaptation of *Enterococcus faecalis* to daptomycin reveals an ordered progression to resistance. Antimicrob Agents Chemother 57:5373–5383. https://doi.org/10.1128/AAC.01473-13.
22. Beabout K, Hammerstrom TG, Wang TT, Bhatty M, Christie PJ, Saxer G, Shamoo Y. 2015. Rampant parasexuality evolves in a hospital pathogen during antibiotic selection. Mol Biol Evol 32:2585–2597. https://doi.org/10.1093/molbev/msv133.
23. Mehta H, Weng J, Prater A, Elworth RAL, Han X, Shamoo Y. 2018. Pathogenic *Nocardia cyriacigeorgica* and *Nocardia nova* evolve to resist trimethoprim-sulfamethoxazole by both expected and unexpected pathways. Antimicrob Agents Chemother 62:00364-18. https://doi.org/10.1128/AAC.00364-18.
24. Mehta HH, Prater AG, Shamoo Y. 2018. Using experimental evolution to identify druggable targets that could inhibit the evolution of antimicrobial resistance. J Antibiot (Tokyo) 71:279–286. https://doi.org/10.1038/ja.2017.108.
25. Toprak E, Veres A, Michel J-B, Chait R, Hartl DL, Kishony R. 2012. Evolutionary paths to antibiotic resistance under dynamically sustained drug selection. Nat Genet 44:101–105. https://doi.org/10.1038/ng.1034.
26. Cabot G, Zamorano L, Moyà B, Juan C, Navas A, Blázquez J, Oliver A. 2016. Evolution of *Pseudomonas aeruginosa* antimicrobial resistance and fitness under low and high mutation rates. Antimicrob Agents Chemother 60:1767–1778. https://doi.org/10.1128/AAC.02676-15.
27. Moskowitz SM, Brannon MK, Dasgupta N, Pier M, Sgambati N, Miller AK, Selgrade SE, Miller SI, Denton M, Conway SP, Johansen HK, Høiby N. 2012. PmrB mutations promote polymyxin resistance of *Pseudomonas aeruginosa* isolated from colistin-treated cystic fibrosis patients. Antimicrob Agents Chemother 56:1019–1030. https://doi.org/10.1128/AAC.05829-11.
28. Lee JY, Park YK, Chung ES, Na IY, Ko KS. 2016. Evolved resistance to colistin and its loss due to genetic reversion in *Pseudomonas aeruginosa*. Sci Rep 6:25543. https://doi.org/10.1038/srep25543.
29. Clinical and Laboratory Standards Institute (CLSI). 2017. Performance standards for antimicrobial susceptibility testing, 27th ed. CLSI supplement M100. Clinical and Laboratory Standards Institute, Wayne, PA.
30. Oliver A, Baquero F, Blázquez J. 2002. The mismatch repair system (*mutS, mutL* and *uvrD* genes) in *Pseudomonas aeruginosa*: molecular characterization of naturally occurring mutants. Mol Microbiol 43:1641–1650. https://doi.org/10.1046/j.1365-2958.2002.02855.x.
31. McPhee JB, Lewenza S, Hancock REW. 2003. Cationic antimicrobial peptides activate a two-component regulatory system, PmrA-PmrB, that regulates resistance to polymyxin B and cationic antimicrobial peptides in *Pseudomonas aeruginosa*. Mol Microbiol 50:205–217. https://doi.org/10.1046/j.1365-2958.2003.03673.x.
32. Moskowitz SM, Ernst RK, Miller SI. 2004. PmrAB, a two-component regulatory system of *Pseudomonas aeruginosa* that modulates resistance to cationic antimicrobial peptides and addition of aminoarabinose to lipid A. J Bacteriol 186:575–579. https://doi.org/10.1128/JB.186.2.575-579.2004.
33. Lee JY, Ko KS. 2014. Mutations and expression of PmrAB and PhoPQ related with colistin resistance in *Pseudomonas aeruginosa* clinical isolates. Diagn Microbiol Infect Dis 78:271–276. https://doi.org/10.1016/j.diagmicrobio.2013.11.027.
34. Barrow K, Kwon DH. 2009. Alterations in two-component regulatory systems of *phoPQ* and *pmrAB* are associated with polymyxin B resistance in clinical isolates of *Pseudomonas aeruginosa*. Antimicrob Agents Chemother 53:5150–5154. https://doi.org/10.1128/AAC.00893-09.
35. Pamp SJ, Gjermansen M, Johansen HK, Tolker-Nielsen T. 2008. Tolerance to the antimicrobial peptide colistin in *Pseudomonas aeruginosa* biofilms is linked to metabolically active cells, and depends on the *pmr* and *mexAB-oprM* genes. Mol Microbiol 68:223–240. https://doi.org/10.1111/j.1365-2958.2008.06152.x.
36. Han M, Velkov T, Zhu Y, Roberts KD, Le Brun AP, Chow SH, Gutu AD, Moskowitz SM, Shen H, Li J. 2018. Polymyxin-induced lipid A deacylation in *Pseudomonas aeruginosa* perturbs polymyxin penetration and confers high-level resistance. ACS Chem Biol 13:121–130. https://doi.org/10.1021/acschembio.7b00836.
37. Barrick JE, Yu DS, Yoon SH, Jeong H, Oh TK, Schneider D, Lenski RE, Kim JF. 2009. Genome evolution and adaptation in a long-term experiment with *Escherichia coli*. Nature 461:1243–1247. https://doi.org/10.1038/nature08480.
38. Gullberg E, Cao S, Berg OG, Ilback C, Sandegren L, Hughes D, Andersson DI. 2011. Selection of resistant bacteria at very low antibiotic concentrations. PLoS Pathog 7:e1002158. https://doi.org/10.1371/journal.ppat.1002158.
39. Oliveira dos Santos S, Martins La Rocca S, Hörner R. 2016. Colistin resistance in non-fermenting Gram-negative bacilli in a university hospital. Braz J Infect Dis 20:649–650. https://doi.org/10.1016/j.bjid.2016.08.009.
40. Ramesh N, Prasanth M, Ramkumar S, Suresh M, Tamhankar AJ, Gothandam KM, Karthikeyan S, Bozdogan B. 2016. Colistin susceptibility of Gram-negative clinical isolates from Tamil Nadu, India. Asian Biomed 10:35–39.
41. Denton M, Kerr K, Mooney L, Keer V, Rajgopal A, Brownlee K, Arundel P, Conway S. 2002. Transmission of colistin-resistant *Pseudomonas aeruginosa* between patients attending a pediatric cystic fibrosis center. Pediatr Pulmonol 34:257–261. https://doi.org/10.1002/ppul.10166.
42. Rojo-Molinero E, Macià MD, Oliver A. 2019. Social behavior of antibiotic resistant mutants within *Pseudomonas aeruginosa* biofilm communities. Front Microbiol 10:570. https://doi.org/10.3389/fmicb.2019.00570.
43. Swings T, Weytjens B, Schalck T, Bonte C, Verstraeten N, Michiels J, Marchal K. 2017. Network-based identification of adaptive pathways in evolved ethanol-tolerant bacterial populations. Mol Biol Evol 34:2927–2943. https://doi.org/10.1093/molbev/msx228.
44. Joshi NA, Fass JN. 2011. Sickle: a sliding-window, adaptive, quality-based trimming tool for FastQ files (version 1.33). https://github.com/najoshi/sickle.
45. Deatherage DE, Barrick JE. 2014. Identification of mutations in laboratory evolved microbes from next-generation sequencing data using breseq. Methods Mol Biol 1151:165–188. https://doi.org/10.1007/978-1-4939-0554-6_12.
46. Kumar S, Stecher G, Tamura K. 2016. MEGA7: Molecular Evolutionary

Genetics Analysis version 7.0 for bigger datasets. Mol Biol Evol 33:1870–1874. https://doi.org/10.1093/molbev/msw054.
47. Nei M, Kumar S. 2000. Molecular evolution and phylogenetics. Oxford University Press, Oxford, United Kingdom.
48. Huson DH, Scornavacca C. 2012. Dendroscope 3: an interactive tool for rooted phylogenetic trees and networks. Syst Biol 61:1061–1067. https://doi.org/10.1093/sysbio/sys062.
49. Winsor GL, Griffiths EJ, Lo R, Dhillon BK, Shay JA, Brinkman FSL. 2016. Enhanced annotations and features for comparing thousands of *Pseudomonas* genomes in the *Pseudomonas* genome database. Nucelis Acids Res 44:D646–D653. https://doi.org/10.1093/nar/gkv1227.
50. Huang W, Wilks A. 2017. A rapid seamless method for gene knockout in *Pseudomonas aeruginosa*. BMC Microbiol 17:199. https://doi.org/10.1186/s12866-017-1112-5.
51. Bhate MP, Molnar KS, Goulian M, DeGrado WF. 2015. Signal transduction in histidine kinases: insights from new structures. Structure 23:981–994. https://doi.org/10.1016/j.str.2015.04.002.
52. Schurek KN, Sampaio JL, Kiffer CR, Sinto S, Mendes CM, Hancock RE. 2009. Involvement of *pmrAB* and *phoPQ* in polymyxin B adaptation and inducible resistance in non-cystic fibrosis clinical isolates of *Pseudomonas aeruginosa*. Antimicrob Agents Chemother 53:4345–4351. https://doi.org/10.1128/AAC.01267-08.
53. Billings N, Millan MR, Caldara M, Rusconi R, Tarasova Y, Stocker R, Ribbeck K. 2013. The extracellular matrix component Psl provides fast- acting antibiotic defense in *Pseudomonas aeruginosa* biofilms. PLoS Pathog 9:e1003526. https://doi.org/10.1371/journal.ppat.1003526.
54. Lee J, Chung ES, Na IY, Kim H, Shin D, Ko KS. 2014. Development of colistin resistance in *pmrA-*, *phoP-*, *parR-* and *cprR*-inactivated mutants of Pseudomonas aeruginosa. J Antimicrob Chemother 69:2966–2971. https://doi.org/10.1093/jac/dku238.
55. Hoang TT, Karkhoff-Schweizer RR, Kutchma AJ, Schweizer HP. 1998. A broad-host-range Flp- FRT recombination system for site-specific excision of chromosomally-located DNA sequences: application for isolation of unmarked *Pseudomonas aeruginosa* mutants. Gene 212:77–86. https://doi.org/10.1016/S0378-1119(98)00130-9.